



## Comparative study on CAS, UCT, and MBR configurations for nutrient removal from hospital wastewater

Faris H. Al-Ani<sup>a</sup>, Hasan Sh. Majdi<sup>b</sup>, Jamal M. Ali<sup>c</sup>, Ayham M. Al Rahawi<sup>d</sup>, Qusay F. Alsalhy<sup>c</sup>

<sup>a</sup>Civil Engineering Department, University of Technology, Alsinaa Street 52, Baghdad, Iraq, email: farishamodi@yahoo.com (F.H. Al-Ani)

<sup>b</sup>Chemical Engineering and Oil Refinery Department, AlMustaqbal University College, Hilla, Babylon, Iraq, email: hasanshker1@gmail.com (H.Sh. Majdi)

<sup>c</sup>Membrane Technology Research Unit, Chemical Engineering Department, University of Technology, Alsinaa Street 52, Baghdad, Iraq, email: jmal\_ali2003@yahoo.com, 80002@uotechnology.edu.iq, (J.M. Ali), Tel. +9647901730181, email: qusay\_alsalhy@yahoo.com, 80006@uotechnology.edu.iq (Q.F. Alsalhy)

<sup>d</sup>Department of Engineering, German University of Technology (GUtech), Muscat, Oman, email: ayham.alrahawi@gutech.edu.om (A.M. Al Rahawi)

Received 9 November 2018; Accepted 22 May 2019

### ABSTRACT

In the present study, treatment of hospital wastewater by processes based on different configurations, such as conventional activated carbon (CAS), University of Cape Town (UCT), and membrane bioreactor (MBR), was explored under the same operational conditions. The findings indicated that MBR was significantly more efficient than CAS and UCT in the removal of the total suspended solids (TSS). The MBR removal efficiency reached nearly 100% during the time designated for this process, whereby the remaining effluent quantity was below 1 mg/l. The difference in the expulsion efficiencies of the three studied configurations was attributed to the evacuation of the chemical oxygen demand (COD) using the membrane and MLSS, which was present in high concentration in the MBR system. Generally, MBRs are efficient at disposing COD through membrane separation in hospital wastewater treatment. In the experiments, NH<sub>3</sub> removal rate of 38.13% was noted for CAS, while 84.98% was obtained for the UCT configuration, and 43.75% was measured for the MBR system when the hydraulic retention time (HRT) = 8 h and solid retention time (SRT) = 25 d. The effluent water quality of MBR system remained stable and was not affected by fluctuations in the influent quality, which was not the case for the CAS system.

*Keywords:* Flat-sheet membrane; PVC; Wastewater treatment; CAS; UCT; MBR

### 1. Introduction

Wastewater containing elevated amounts of phosphorus and nitrogen can cause considerable issues, especially for the soil, as it affects oxygen utilization, eutrophication and poisonous quality. Thus, several biological nutrient removal (BNR) processes have been established for the removal these elements from wastewater [1].

Among the currently utilized wastewater treatment procedures, configurations based on BNR, conventional activated carbon (CAS), University of Cape Town (UCT), and membrane bioreactor (MBR) are the most popular [1–5]. The activated sludge (AS) process derives its name from the natural mass that is formed when air is infused into the wastewater. In this procedure, microorganisms are mixed with the characteristic blends contained in wastewater. As the biomass develops and is blended by the agitation of air, the individual living beings floccu-

\*Corresponding author.

late to shape a dynamic mass of organisms (biologic floc) called activated sludge. The UCT procedure was created to reduce the impact of nitrate in wastewater upon its release into an anaerobic zone. The nitrate amount in the zone of anaerobic process is crucial for the natural phosphorus evacuation effectiveness. The procedure of UCT is like the  $A_2O$  procedure with two special cases, as the AS is reused in the stage of anoxic process, rather than the stage of aeration process, and the inside reuse is from the anoxic stage to the anaerobic stage. Combining BNR with MBR can meet strict nutrient release principles. The system of MBR combines an organic treatment operation together with a microfiltration or ultrafiltration membrane, which results in high emanating quality, high treatment productivity, high adaptability, and low sludge production.

BNR incorporates the expulsion of excess phosphorus and nitrogen remaining after biomass generation [6]. Nitrogen expulsion is a procedure comprising of nitrate formation by nitrification of  $NH_3$ , which is in turn denitrified to nitrogen gas before being expelled from the processing unit. The expulsion of nitrogen by microscopic organisms from wastewater occurs in nitrification stage followed by denitrification stage. Nitrification is a biochemical procedure comprising of  $NH_3$  oxidation into  $NO_3^-$  via nitrite  $NO_2^-$ .

The outputs from this process are microscopic organisms such as nitrite-oxidizing bacteria (NOB) and ammonia-oxidizing bacteria (AOB). NOB oxidize nitrite into nitrate, while AOB oxidize ammonia into nitrite. The two AOB genera—*Nitrosomonas* and *Nitrospira*—are usually present in MBR plants, whereas the two typical NOB genera are *Nitrobacter* and *Nitrospira*.

Denitrification is the microbiological operation by which nitrate ( $NO_3^-$ ) is changed into nitrogen gas ( $N_2$ ) by means of sequential reduction methods including dinitrogen oxide ( $N_2O$ ), nitric oxide (NO), and nitrite ( $NO_2^-$ ). An organic phosphorus evacuation operation uses bacterial capacities for their ability to take up phosphorus. Therefore, this method is considered enhanced biological removal of phosphorus (P). The microorganisms that are required for this operation are denoted as phosphate-accumulating organisms (PAOs) [6,7]. In anaerobic states characterized by few DO contents, PAOs promptly change accessible organic compounds, such as volatile fatty acids, to carbon mixes, yielding polyhydroxybutyrate (PHB) and polyhydroxyalkanoates (PHA). The consequence of this process is a primary remove of P from the cells as reported by several researchers [8–10]. For the zones of aerobic with elevated DO contents, carbon is utilized by PAOs for development of biomass and formation of polyphosphate (Poly-P) [9,11]. For productive P evacuation, it is critical in the bioreactor to advance the development of PAOs, which can be hindered by denitrifies or existence of nitrate. Our previous work focused on the preparation of PVC/ZnO-NPs with 13 wt.% PVC and various NPs contents and its application on the treatment of actual hospital wastewater [12]. In addition, suggested MBR design in which a composite layer prepared from Sponge/Granular Activated Carbon/Sponge kept in front of the membrane surface works as a pre-filter in hospital wastewater treatment in order to minimize the antifouling on the mem-

brane surface [13]. This study investigates the difference in removal efficiency between various pilot plants while using the same water source, same operating conditions and similar wastewater characteristics. The study aims on providing an understanding of the complex biological phenomena that mediate nutrient removal processes in MBR BNR systems. In addition, the study quantifies the kinetics of the biologically mediated processes of nutrient removal in these systems. Furthermore, the study will discuss the different means used for the treatment of hospital wastewater. Therefore, the objective of this effort was to compare the removal efficiency of different CAS, UCT, and MBR process configurations in terms of COD, phosphorus, nitrogen, and total suspended solids (TSS) concentrations, under the same organic load and hydrodynamic conditions.

## 2. Material and methods

### 2.1. Material

PVC resins with 65 kg/mol were purchased from the Georgia Gulf Company (Georgia, USA) and the dimethylacetamide (DMAc) used as a solvent was purchased from Sigma-Aldrich, Germany. The granular activated carbon (GAC) was purchased from ROMIL PURE CHEMISTRY, Cambridge GB-CB259QT. ZnO nanoparticles (product no. 8411DL, 99%, 10–30 nm) were purchased from Sky Spring Nanomaterials, Inc. USA.

### 2.2. PVC membrane

PVC membrane material was kept for 4 h in an oven at 60°C for moisture removal. The dried 10 wt.% PVC was added to 90 wt.% DMAc with continuous mixing at 40°C, by using a magnetic stirrer at 200 rpm for 2 d, until homogeneity was accomplished. Next, 0.1 g of ZnO nanoparticles (NPs) was combined with the polymer solution to prevent sedimentation. After that, the homogeneous PVC solution with ZnO-NPs was kept for 25 min in an ultrasonic water bath to avoid agglomeration of ZnO nanoparticles. The PVC casting solutions were cast with knife thickness of 180  $\mu m$  using a motorized film applicator (CX4 mtvmesstechnik, Germany). Next, the nascent flat-sheet membranes were immersed in coagulation bath containing deionized water at laboratory temperature. The PVC-NPs membrane was subsequently submerged under deionized water for 48 h to complete DMAc removal. Then, the membrane was kept for 48 h in a 30/70 wt.% glycerol-water solution to prevent its structure from cracking and crumpling.

The specification and membrane structure with pore size distribution of the membrane prepared in this work are presented in Table 1 and Fig. 1.

### 2.3. Membrane performance

Pollutant removal and water permeation flux for the membranes were assessed via cross-flow filtration method.

Table 1  
Specification of the PVC/ZnO-NPS membrane

Membrane specification	Value
PVC	10 wt.%
ZnO-NPS	0.1 gm
Thickness	47.45 $\mu\text{m}$
Porosity	88%
Average pore size	211.32 nm
$\leq 90\%$ pore size	300.00 nm
$\leq 50\%$ pore size	180.00 nm

The separation performance was conducted using a membrane module at a 0.4 bar vacuum and a feed solution at a temperature of 25°C. The solution volume was 5 l and the membrane effective surface area was 18 cm<sup>2</sup>. Graduated cyl-

inder was used as a permeate collector. Pure water permeability (PWP) was estimated by using the following formula:

$$PWP = \frac{V}{t \cdot A \cdot P} \quad (1)$$

where  $V$  denotes the collected volume (l),  $P$  is the trans-membrane pressure (Pa),  $A$  represents the membrane surface area (m<sup>2</sup>) and  $t$  is the permeate collection time (h).

The dissolved pollutant removal efficiency  $R$  (%) was estimated according to the following equation:

$$R(\%) = \left(1 - \frac{C_p}{C_f}\right) \times 100 \quad (2)$$

where  $C_p$  and  $C_f$  represent the pollutant concentrations of the effluent and influent, respectively.

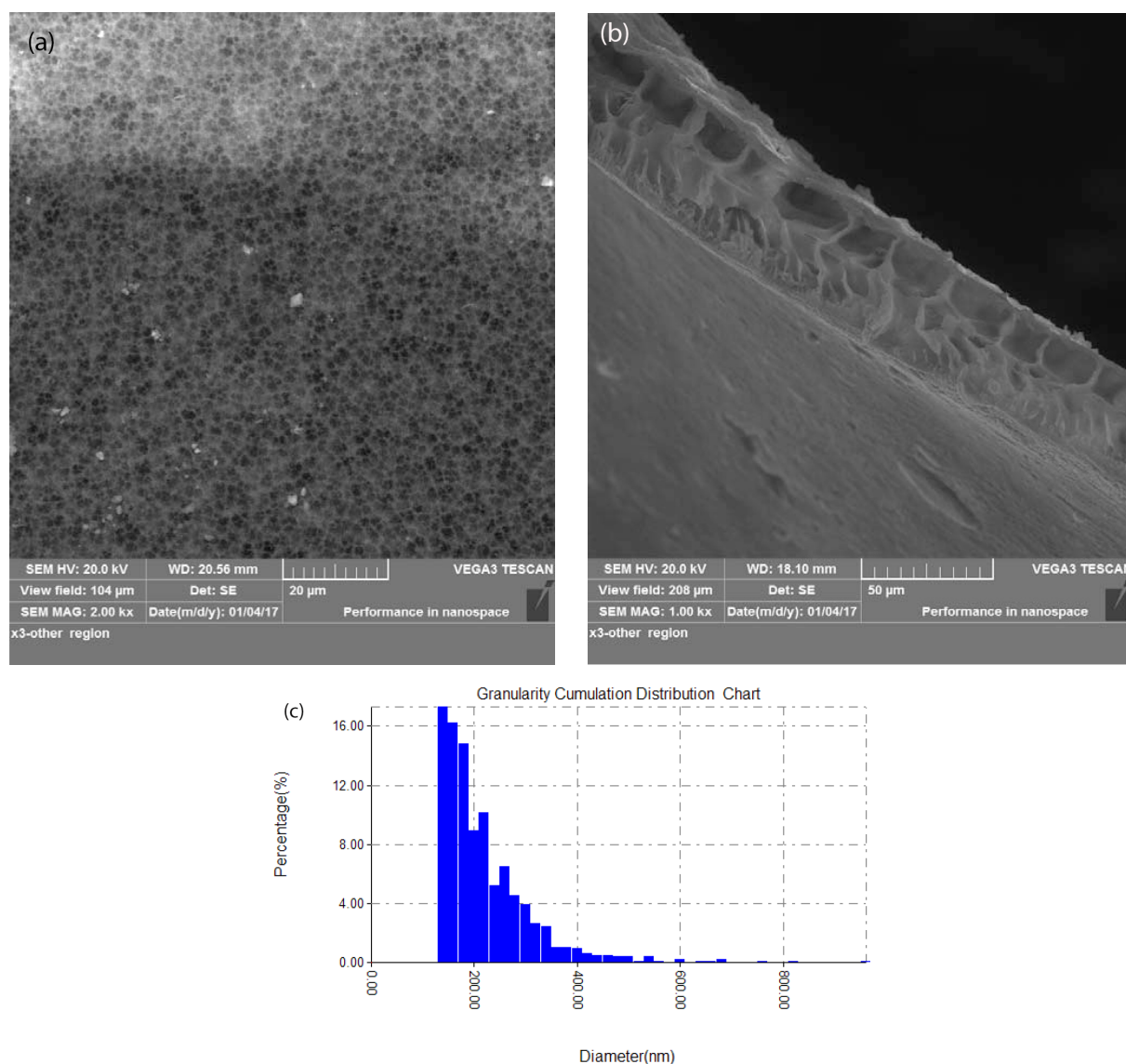


Fig. 1. SEM images and pore size distribution of PVC/ZnO-NPs membrane prepared from PVC of 10%, and ZnO-NPs of 0.1 gm.

#### 2.4. Experimental rig

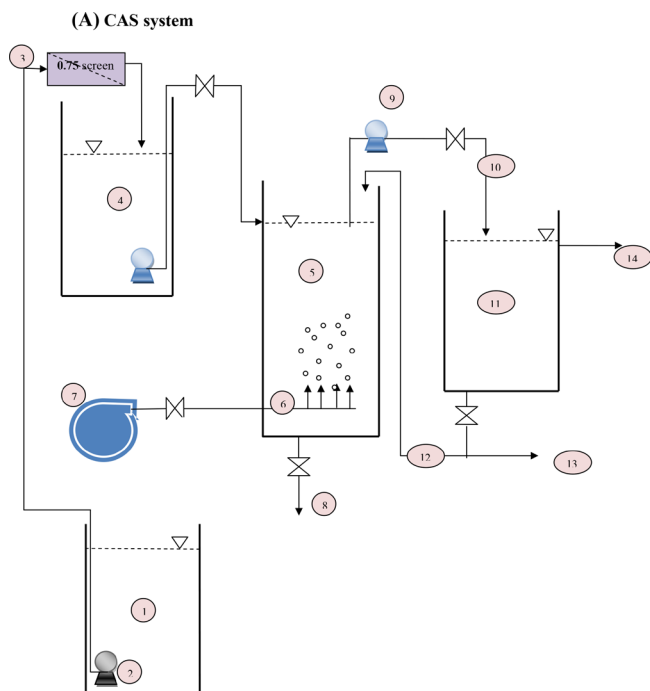
The experiments were conducted in three pilot plants, which were fed real hospital wastewater from a capacity tank by means of a sustained suction pump. The real hospital wastewater was collected from a discharge of wastewater treatment plant (WWTP) located in Hilla Hospital south of Iraq.

As shown in Fig. 2a, in one of the pilot plants a CAS was implemented. The CAS system consisted of four major components, namely influent tank, aerobic bioreactor, aeration system and settling tank. The influent tank, which has an overall working volume of 80 l, is made of glass, and was fitted with one nozzle for wastewater feed and maintenance. Wastewater level in this tank was controlled by an electrical float connected with submersible pump located in the hospital wastewater collection basin. The bioreactor used had a 32 l capacity. Real wastewater was pumped to the reactor via a feeding pump to precisely determine the feed rate, whereas the effluent flow rate was controlled by a suction pump. In order to control and measure the wastewater volume in the reactor, level sensors were fitted. The reactor contained four nozzles of  $\varnothing 15$  mm each, three of which were at the same side, whereby one was located at the top to receive wastewater and two were positioned at the bottom for sludge removal and air feed. The fourth nozzle was located on the opposite side to transfer sludge to the settling tank of 60 l capacity, made of acrylic sheet. This tank was fitted with two nozzles of 15 and 20 mm diameter, both of which were placed at the top to receive MLSS from the aerobic bioreactor and to discharge effluent water, respectively. Another nozzle of 15 mm diameter was placed at the bottom for sludge removal. The purpose of this tank was to separate solids from water in order to provide clear effluent containing allowable limits of suspended solids and colloidal particles.

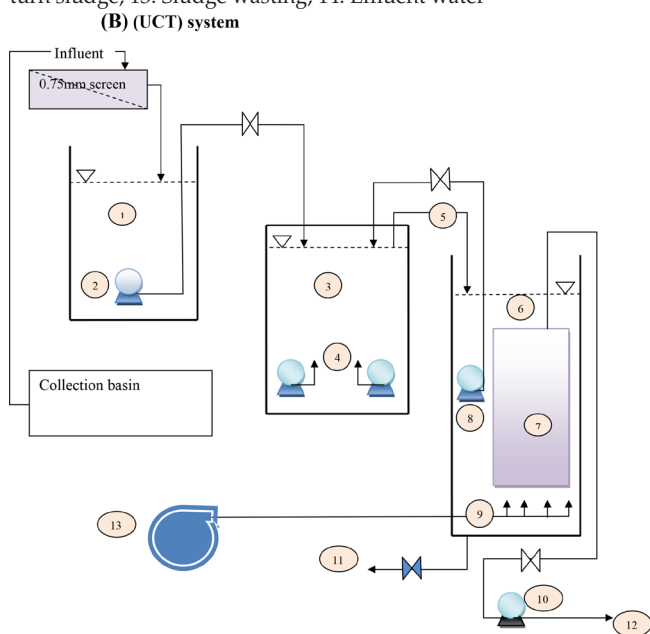
As shown in Fig. 2b, in one of the pilot plants UCT was adopted, comprising of an aerobic tank (32 l), an anoxic tank (16 l) and anaerobic tank (8 l). In the aerobic tank, air was injected from the bottom of the tank to provide oxygen required by the microorganisms. Both the anoxic and the anaerobic tank were fitted with a stirrer. From the aerobic tank, the mixed liquors were recycled

Table 2  
Characteristics of hospital wastewater

Pollutant	Influent concentration (mg/l)	Max. allowable limit (mg/l)
COD	800–1200	100
NH <sub>3</sub>	140–190	–
NO <sub>3</sub>	45–100	50
P	12–18	3
TSS	–	–
CL	260	100
Pb	0.004	0.05
cd	0.0023	0.1
pH	7.2	6.5–8.5



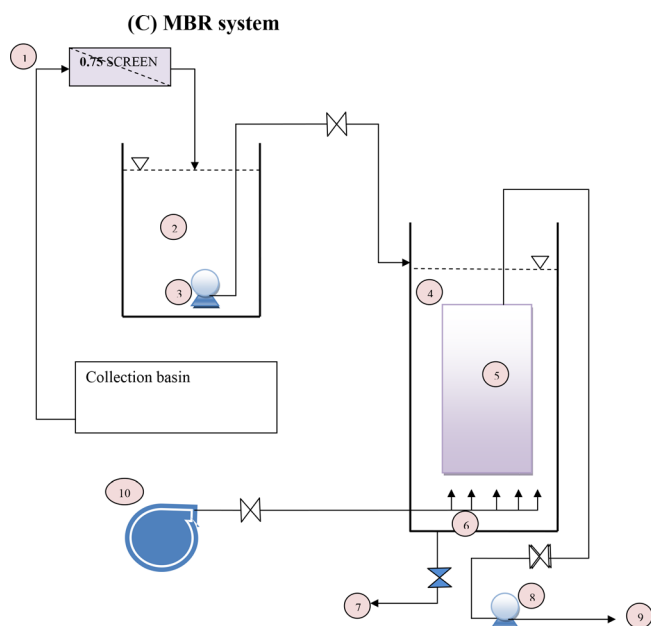
1. Collection basin, 2. Submersible pump, 3. Influent, 4. Influent tank, 5. Aerobic bioreactor, 6. Air diffuser, 7. Air compressor, 8. Drain valve, 9. Submersible pump, 10. MLSS feed, 11. Settling tank, 12. Return sludge, 13. Sludge wasting, 14. Effluent water



1. Anaerobic bioreactor, 2. Submersible pump, 3. Anoxic bioreactor, 4. Submersible pump for homogenization, 5. Sludge returning, 6. Aerobic bioreactor, 7. FS membrane module, 8. Submersible pump for recirculation, 9. Air diffuser, 10. Suction pump, 11. Sludge wasting, 12. Permeate, 13. Air compressor,

Fig. 2. A schematic diagram of the lab scale of three different configurations.

to the anoxic tank (Loop 1). After that, the mixed liquors were moved to the anaerobic tank (Loop 2) using two pumps. Real wastewater was transferred from the stor-



1. Influent, 4. Aerobic bioreactor, 7. Sludge wasting, 10. Air compressor, 2. Influent tank, 5. Flat sheet (FS) membrane, 8. Suction pump, 3. Submersible pump, 6. Air diffuser, 9. Permeate, 10. Air compressor

Fig. 2. Continued.

age tank to the anaerobic tank. In the chamber designated for the anaerobic process, phosphorus was released and the COD was partially consumed. Next, the effluent was transferred to the MBR and anoxic tank. Nitrification, phosphorus accumulation, and organic matter oxidation take place in the zones of aerobic operation. Loop 1 composed of  $\text{NO}_3^-$  returned to the bioreactor anoxic chamber from the membrane tank, in order to decrease the effect of nitrate in wastewater coming from the zone of anaerobic. As a part of Loop 2, the wastewater from anoxic chamber was returned to the anaerobic tank to enhance the organic matter utilization and provide the best conditions for P uptake in the tank of anaerobic operation, as well as facilitate fermentation of organic material.

Fig. 2c shows a schematic of the MBR system with effective volume of the bioreactor of about 32 l. As a part of this process, real wastewater was transferred into the reactor to control the feed rate via a feeding pump, whereas the flow rate of the effluent was determined by a suction pump. In order to control the volume of the wastewater in the tank, level sensor was utilized. To supply oxygen for microorganisms, at the bottom of the aerobic tank air was injected, and the TMP gauge was used to measure pressure. The MBR was filled with sludge from the local WWTP and adapted to real wastewater.

### 2.5. Operating conditions of the process

Activated sludge was sourced from the aeration tank of the existing conventional wastewater treatment unit of Al-Rustumia Treatment Plant, Baghdad. It was used as microorganism seeding for the system examined in the present study. Actual wastewater was obtained down-

stream from the wastewater treatment plant located in Babylon Hospital (Babylon province, Iraq). After the activated sludge was concentrated by settling to about  $1.5 (\pm 0.09)$  g/l MLSS, the system was fed with wastewater until the steady state of  $8.8 (\pm 1.1)$  g/l of MLSS was achieved. While evaluating the UCT configuration, the dissolved oxygen (DO) concentration was kept within 4 mg/l in the aerobic tank, 0.2 mg/l in the anoxic tank, and  $< 0.1$  mg/l in the anaerobic tank. The temperature of mixed liquor was continuously monitored and was kept within the  $25 \pm 2^\circ\text{C}$  range by a temperature controller. The internal recycle rate was maintained at 300% and 100% of the influent flow rate. The filtration mode with intermittent time, for example, 10 min suction followed by relaxation (non-suction) for 1 min, was controlled. The HRT was kept at 8 h, whereas a series of SRTs were controlled over a period of 25 d. The operating conditions and working MLSS contents in this investigation are reported in Table 3.

### 2.6. Analytical methods

#### 2.6.1. Total suspended solids (TSS)

The total suspended solids (TSS) analyses were conducted utilizing the procedures prescribed by APHA (2012) [14], as shown in Fig. 3. Briefly, volume of test sample was separated through a pre-measured Glass Microfibre Filters with pore size of  $0.45 \mu\text{m}$ . Then, each filter was dried at  $105^\circ\text{C}$  in the oven for 2 h and was left to cool to room temperature before being assessed utilizing gravimetric strategy for TSS.

#### 2.6.2. COD

The COD assessments were performed in the Environmental Research Center, University of Technology-Baghdad, utilizing the strategies reported by APHA (2012) [14]. COD VARIO Photometer, Lovibond, Germany was utilized to measure the COD content. For influent digestion solution with high content was utilized, whereas for

Table 3  
Operation conditions and working concentration of MLSS in the steady state for CAS, UCT, and MBR system

Parameter		Run 1 CAS	Run 2 UCT	Run 3 MBR
Volume (L)	Anaerobic	0	8	0
	Anoxic	0	16	0
	Aerobic	32	32	32
HRT (h)	Anaerobic	2	0	0
	Anoxic	4	0	0
	Aerobic	8	8	8
SRT (d)		25	25	25
MLSS (mg/l)		10000	10000	10000
Vacuum (bar)		0.4	0.4	0.4
Operation time (d)		21	21	21

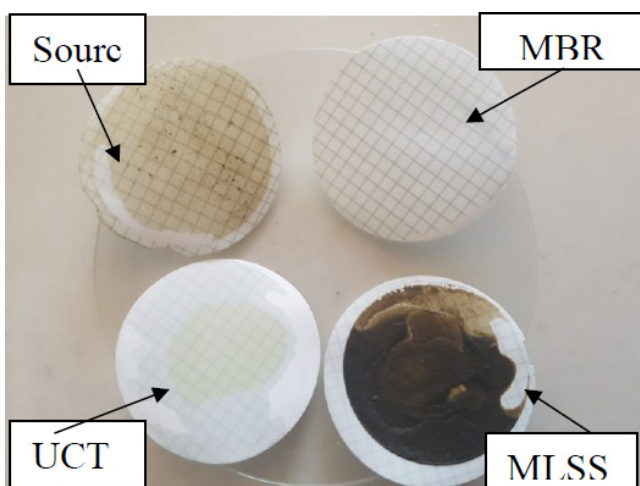


Fig. 3. TSS & MLSS test.

effluent, digestion solution with moderate content was adopted, and distilled water served as blank samples. At 150°C the test tubes were heated for 2 h and were subsequently permitted to cool to 25°C before spectrometer readings were taken.

### 2.6.3. Content of dissolved oxygen (DO)

YSI, Model 556, USA DO Meter was used to measure the DO concentration. In the aerobic bioreactor, DO concentration was constantly monitored with the DO meter, whereas the flow rate of the air was regulated manually by setting the value of the input air. Unless otherwise stated, the DO content in the zones of anoxic, anaerobic, and aerobic was maintained respectively at <0.2 mg/l, <0.1 mg/l, and 1–4 mg/l.

#### 2.6.3.1. NH<sub>3</sub>

Multi-parameter photometer (C200 & HI 83200, Germany) was used for the measurements of P, NO<sub>2</sub>, NO<sub>3</sub>, and NH<sub>3</sub>.

## 3. Results and discussion

### 3.1. PVC/ZnO-NPs membrane morphology and specification

The structural morphology of the PVC/ZnO-NPS membrane cross-section and top surface was examined via SEM and AFM. Fig. 1a shows that the PVC/ZnO-NPS membrane cross-section comprises of two layers characterized by spherical and finger-like structures. In addition, the SEM image of the PVC/ZnO-NPS membrane top surface shown in Fig. 1b reveals that the surface is skinless and porous, and is thus suitable for application in the MBR process. The addition of ZnO NPs into the dope solution has a strong effect on the phase inversion process and finally on membrane morphology [15,16]. In addition, these nanoparticles decrease the interaction between polymer and solvent. Therefore, solvent can diffuse more easily from then ascent membrane into water, and phase inversion occurs faster [17]. The maximum removal efficiency for the components suspended in the wastewater is attributed to this preferred porous structure, which has minimal effect on the membrane permeation flux. For this reason, 10 wt.% PVC was adopted as the membrane material and 0.1 g of ZnO was selected as the most optimal choice of anti-fouling nanoparticles. This phenomenon is because of the delayed solvent-nonsolvent demixing process between the solvent in polymer solution and the water (non-solvent) owing to the presence of ZnO nanoparticles in the polymer solution. Yang et. al. [18] reported that at low nanoparticle concentration, the macro-voids grow and become run-through and at higher nanoparticle concentration are suppressed. This phenomenon indicates an important effect of ZnO nanoparticles in polymer solution on the membrane structure. Fig. 1c shows the pore size distribution yielded by the PVC/ZnO-NPS membrane top surface AFM analysis.

### 3.2. TSS removal by CAS, UCT, and MBR

Experiments conducted as a part of the present study are summarized in Fig. 4, whereby TSS concentrations in the effluent and the influent were 162.3 mg/l and 640 mg/l, respectively for the CAS system, whereas the corresponding values in the UCT system were 193.5 and 645 mg/l. For

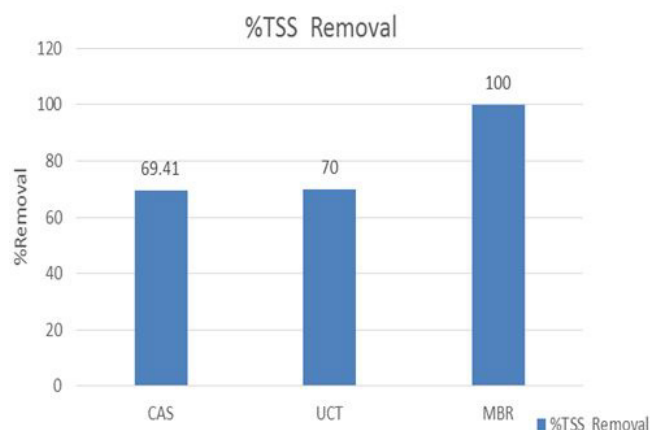


Fig. 4. TSS removal efficiency for CAS, UCT, and MBR experiment.

the MBR system (when the SRT = 25 d and HRT = 8 h), 0 and 636.87 mg/l of TSS was measured in the effluent and influent, respectively. These findings are in line with those reported by other authors, such as Majlesi et. al. and Sarafraz et al. [19,20], who reported the mean TSS removal from hospital wastewater in the 66–87.9% range. In the present study, the MBR was significantly more efficient than CAS and UCT in TSS removal, as it achieved nearly 100% efficacy during the operation time, with less than 1 mg/l of TSS remaining in the effluent.

### 3.3. COD Removal by CAS, UCT, and MBR

For the CAS configuration, Fig. 5 displays the COD removal efficiency and variations in the COD concentration in effluent (Eff.) and influent (Inf.) during the operation time. The COD concentration in influent changed significantly from 800 to 1150 mg/l. However, in the CAS configuration, the expulsion effectiveness was roughly 54.01%. The influent COD concentration in the UCT system was changed from 990 to 1030 mg/l. The COD removal efficiency and change in the COD concentration in influent and effluent during the operation of time are depicted in Fig. 6, indicating that the COD

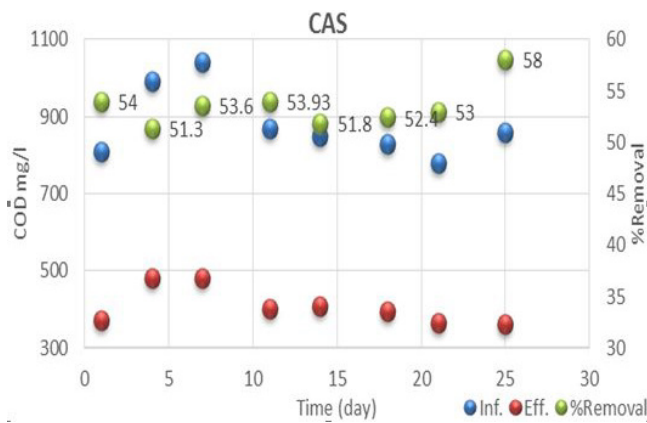


Fig. 5. The influent & effluent COD concentrations and removal efficiency for CAS.

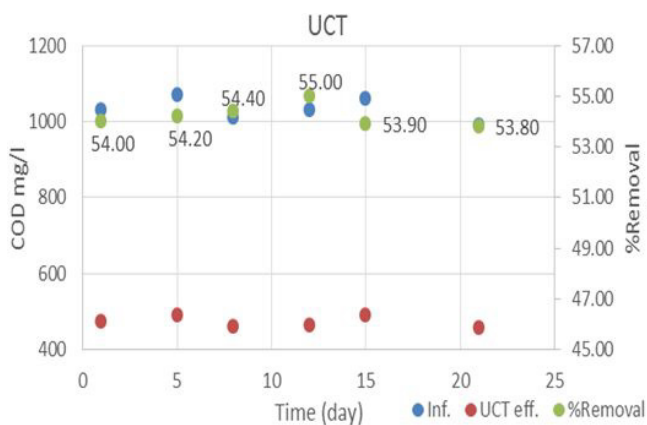


Fig. 6. The influent & effluent COD concentrations and removal efficiency for UCT experiment.

removal efficiency was approximately the same when CAS configuration was utilized due to the same operational conditions.

The COD concentration in the influent during different MBR runs changed from 990 to 1030 mg/l. The removal efficiency of COD and the change in COD concentration in the influent and effluent as a function of time are depicted in Fig. 7. It can be seen that the removal efficiency of COD was approximately 73% for the net PVC membrane. Regardless of operational conditions, the efficiency of COD removal reached over 75%. Adding the membrane significantly contributed to the removal efficiency. This is due to the total retention of all particulate and macromolecular COD components. The results indicated that the membrane could be used to remove COD from wastewater. Alsahy et al. (2018), found that COD removal depending on the structural morphology of membrane [12]. The MBR procedure is typically utilized to expel dissolvable COD [6]. The differences in the expulsion rates obtained from the three configurations (CAS, UCT, and MBR) are a direct result of the high concentration of MLSS and expulsion of the soluble COD by the membrane in the MBR configuration. Katsou et al. [21] reported that the augmentation of vermiculite enhanced the capacity of the framework to oxidize natural issue and diminished the harmful effect of metals on the biomass, which tended to occur a low saturate COD. Thus, MBR remains the most effective COD removal process [22].

### 3.4. Nitrification and denitrification

For the CAS configuration, Fig. 8 shows the NH<sub>3</sub> concentration in the influent and effluent, which ranged from 102.2 to 182.6 mg/l and 66.43 to 118.69 mg/l, respectively. However, the removal efficiency was around 38.13%.

The NH<sub>3</sub> removal in the UCT configuration is demonstrated in Fig. 9. For this configuration, the average NH<sub>3</sub> concentration in the influent was 165.84 mg/l with the average removal efficiency of 84.98%, and 25 mg/l effluent concentration. Fig. 10 shows the NH<sub>3</sub> removal in the MBR configuration, where the average NH<sub>3</sub> average concentration in influent and effluent was 163.54 mg/l and 92.45 mg/l, respectively, with 43.75% average NH<sub>3</sub> removal efficiency.

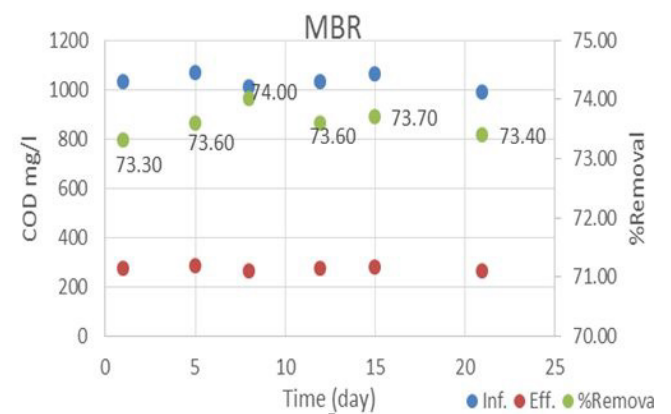


Fig. 7. The influent & effluent COD concentrations and removal efficiency for UCT experiment.

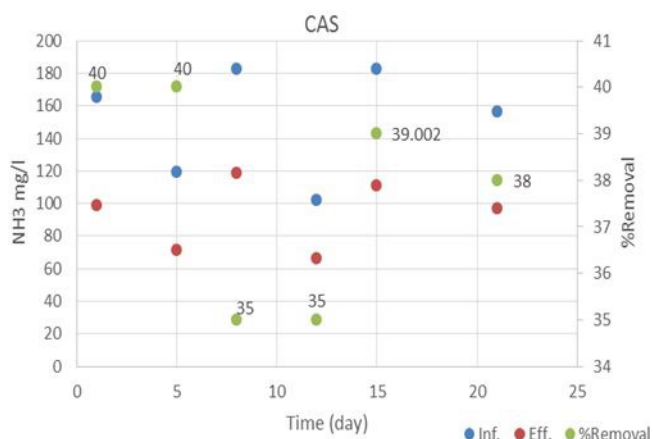


Fig. 8. The influent & effluent NH<sub>3</sub> concentrations and removal efficiency for CAS experiment.

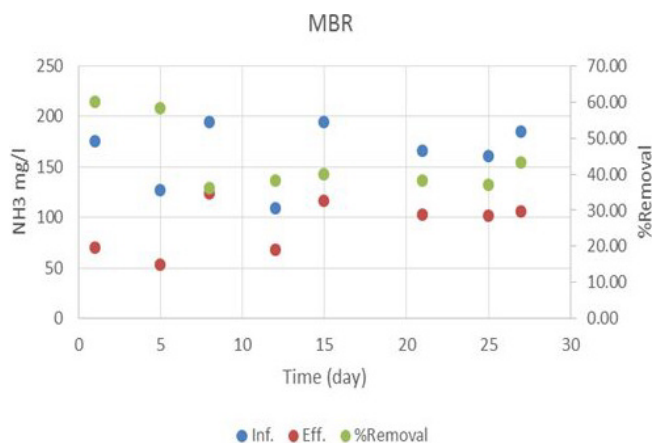


Fig. 10. The influent & effluent NH<sub>3</sub> concentrations and removal efficiency for MBR experiment.

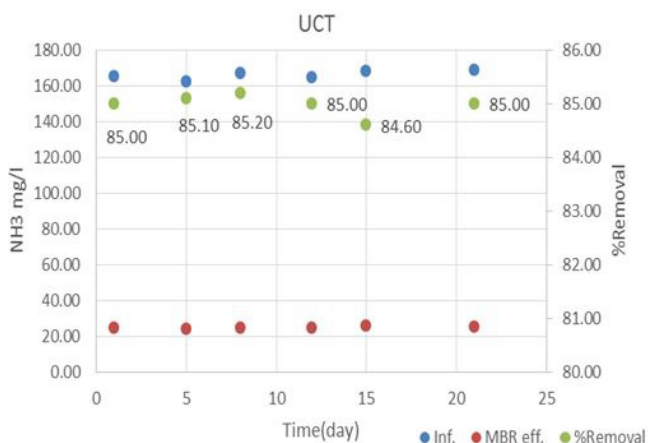


Fig. 9. The influent & effluent NH<sub>3</sub> concentrations and removal efficiency for UCT experiment.

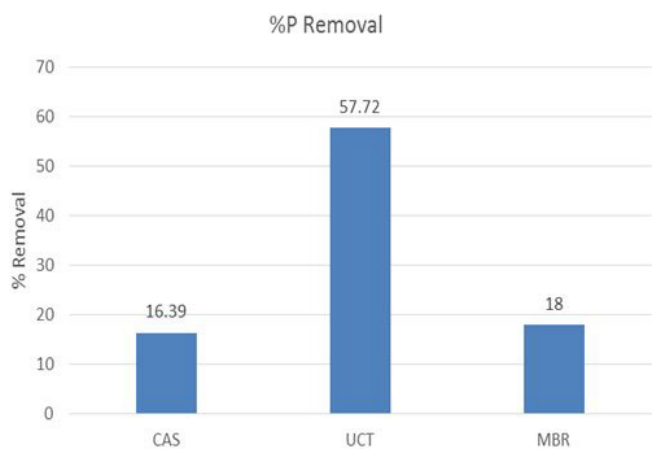


Fig. 11. P removal efficiency for CAS, UCT, and MBR technique.

NH<sub>3</sub> removal in the CAS, UCT and MBR systems was 38.13%, 84.98% and 43.75%, respectively, at HRT = 8 h and SRT = 25 d. These outcomes indicated significant nitrification in the UCT configuration. The internal recycling time mode in UCT configuration represents the ratio of the anoxic period to the anaerobic period. As shown if Fig. 10, UCT has the best removal efficiency in nitrogen. This indicates that both nitrification and denitrification were dependent on the treatment configuration. In fact, the configuration in denitrification performance an important function in the nitrogen removal process [23]. The ammonia removal efficiency might be attributed to an expansion in the MLSS in this configuration, due to which the age of the sludge expanded, enabling the procedure to protect nitrobacteria, yielding the observed nitrification effect, as proposed by Chen et. al. [24].

### 3.5. Phosphorus removal

The performance of each of the three (CAS, UCT, and MBR) configurations was tested for 21 days using a PVC/ZnO-NPs membrane in submerged MBR. Fig. 11 shows the results of the P removal efficiency in three

different configurations, indicating that 16.39%, 18%, and 58% removal was achieved by CAS, MBR, and UCT, respectively.

To attain significant phosphorus removal rates, anaerobic conditions are desired for the take-up and limit of readily biodegradable normal issue and phosphorus release, aggregate phosphate under aerobic or anoxic conditions [25,26]. This phosphorus removal percentage is only applicable to cell metabolisms and growth. This enhanced execution of the MBR would be due to the higher MLSS in this configuration; for example, 8000 mg/l has been reported for MBR versus to 2350 mg/l for CAS. This difference might be due to the effective holding capacity of the PVC/ZnO-NPs membranes, which increased the sludge concentration and enhanced the microbial biomass in reactors, as well as improved the biodegradation capacity of the procedure, as noted by Zheng et al. [27]. In general, the UCT system exhibited good performance to meet the points of confinement for reuse and for release to a specific degree.

### 4. Conclusions

In view of the outcomes obtained in the present study, the following conclusions can be reached:

- The MBR configuration was significantly more efficient than CAS and UCT in TSS removal. The TSS removal efficiency of MBR was nearly 100% during operation time, with the TSS concentration in the effluent remaining below 1 mg/l.
- The differences in the evacuation efficiencies of the CAS, UCT, and MBR configurations are a direct result of the high concentration of MLSS and expulsion of the soluble COD by the membrane in the MBR configuration. Generally, MBRs are efficient at disposing COD through membrane separation in hospital wastewater treatment.
- NH<sub>3</sub> removal in the CAS, UCT, and MBR system was measured at 38.13%, 84.98%, and 43.75%, respectively (at HRT = 8 h and SRT = 25 d).
- The effluent water quality of MBR system remained stable and was not affected by the fluctuations in the influent quality, which was not the case for the CAS system.

## References

- [1] S. Yang, F. Yang, Z. Fu, T. Wang, R. Lei, Simultaneous nitrogen and phosphorus removal by a novel sequencing batch moving bed membrane bioreactor for wastewater treatment, *J. Hazard. Mater.*, 175 (2010) 551–557.
- [2] C. Visvanathan, R.B. Aim, K. Parameshwaran, Membrane separation bioreactors for wastewater treatment, *Crit. Rev. Environ. Sci. Technol.*, 30(1) (2000) 1–48.
- [3] D. Mulkerrins, A. Dobson, E. Colleran, Parameters affecting biological phosphate removal from waste waters, *Environ. Int.*, 30(2) (2004) 249–259.
- [4] D. Mulkerrins, C. Jordan, S. McMahon, E. Colleran, Evaluation of the parameters affecting nitrogen and phosphorus removal in anaerobic/anoxic/oxic(A/A/O) biological nutrient removal systems, *J. Chem. Technol. Biotechnol.*, 75 (2000) 261–268.
- [5] M. Kraume, U. Bracklow, M. Vocks, A. Drews, Nutrient removal in MBRs for municipal wastewater treatment, *Water Sci. Technol.*, 51(6–7) (2005) 391–402.
- [6] Metcalf and Eddy, *Wastewater Engineering: Treatment and Reuse*, Fourth Edition, McGraw Hill Inc., New York, 2003.
- [7] USEPA, *Nutrient Control Design Manual*. State of Technology Review Report; EPA/600/R-09/012; EPA: Cincinnati, Ohio, 2009.
- [8] W.T. Liu, K. Nakamura, T. Matsuo, T. Mino, Internal energy based competition between polyphosphate- and glycogen-accumulating bacteria in biological phosphorus removal reactors—Effect of P/C feeding ratio, *Water Res.*, 31(6) (1997) 1430–1438.
- [9] S. Jeyanayagam, *True Confessions of the Biological Nutrient Removal Process*. Florida Water Resources, 2005, pp. 37–46.
- [10] Y. Liu, Y. Chen, Q. Zhou, Effect of initial pH control on enhanced biological phosphorus removal from wastewater containing acetic and propionic acids, *Chemosphere*, 66 (2007) 123–129.
- [11] J.B. Li, J.W. Zhu, M.S. Zheng, Morphologies and properties of poly (phthalazinone ether sulfone ketone) matrix ultra filtration membranes with entrapped TiO<sub>2</sub> nanoparticles, *J. Appl. Polym. Sci.*, 103 (2007) 3623–3629.
- [12] Q.F. Alsahy, F.H. Al-Ani, A.E. Al-Najar, S. Jabuk, A study of the effect of embedding ZnO-NPs on PVC membrane performance use in actual hospital wastewater treatment by membrane bioreactor, *Chem. Eng. Process. - Process Intensif.*, 130 (2018) 262–274.
- [13] Q.F. Alsahy, F.H. Al-Ani, A.E. Al-Najar, A new Sponge-GAC-Sponge membrane module for submerged membrane bioreactor use in hospital wastewater treatment, *Biochem. Eng. J.*, 133 (2018) 130–139.
- [14] E.W. Rice, R.B. Baird, A.D. Eaton, L.S. Clesceri, *Standard methods for the examination of water and wastewater*, 22<sup>nd</sup> ed., American Public Health Association (APHA), American Water Works Association, Water Environment Federation, 2012.
- [15] N. Maximous, G. Nakhla, W. Wan, K. Wong, Preparation, characterization and performance of Al<sub>2</sub>O<sub>3</sub>/PES membrane for wastewater filtration, *J. Membr. Sci.*, 341 (2009) 67–75.
- [16] J. Huang, K. Zhang, K. Wang, Z. Xie, B. Ladewig, H. Wang, Fabrication of polyethersulfone-mesoporous silica nanocomposite ultra filtration membranes with anti-fouling properties, *J. Membr. Sci.*, 423–424 (2012) 362–370.
- [17] H. Rabiee, M.H.D.A. Farahani, V. Vatanpour, Preparation and characterization of emulsion poly(vinyl chloride) (EPVC)/TiO<sub>2</sub> nanocomposite ultra filtration membrane, *J. Membr. Sci.*, 472 (2014) 185–193.
- [18] Y. Yang, H. Zhang, P. Wang, Q. Zheng, J. Li, The influence of nano-sized TiO<sub>2</sub> fillers on the morphologies and properties of PSF UF membrane, *J. Membr. Sci.*, 288 (2007) 231–238.
- [19] N.M. Majlesi, A. Yazdanbakhsh, Study on wastewater treatment systems in hospitals of Iran. *Iran. J. Environ. Health Sci. Eng.*, 5(3) (2008) 211–215.
- [20] Sh. Sarafraz, M. Khani, K. Yaghmaeian, Quality and quantity survey of hospital waste waters in Hormozgan province. *Iran. J. Environ. Health Sci. Eng.*, 4(1) (2006) 43–50.
- [21] Katsou, E. Malamis, S. Loizidou, Performance of a membrane bioreactor used for the treatment of wastewater contaminated with heavy metals, *Bioresour. Technol.*, 102(6) (2011) 4325–4332.
- [22] K. Yamamoto, M. Hiasa, T. Mahmood, T. Matsuo, Direct solid-liquid separation using hollow fiber membrane in an activated sludge aeration tank, *Water Sci. Technol.*, 21(4–5) (1989) 43–54.
- [23] Y.T. Ahn, S.T. Kang, S.R. Chae, J.L. Lim, S.H. Lee, H.S. Shin, Effect of internal recycle rate on the high-strength nitrogen wastewater treatment in the combined UBF/MBR system, *Water Sci. Technol.*, 51 (2005) 241–247.
- [24] W. Chen, D. Wu, N.W. Zhu, Enhanced ammonia removal and nitrification rate of A/A/O-MBR combined process, *J. Civil Architect. Environ. Eng.*, 32(4) (2010) 90–95.
- [25] S. Puig, M. Coma, H. Monclús, M.C.M. Van Loosdrecht, J. Colprim, M.D. Balaguer, Selection between alcohols and volatile fatty acids as external carbon sources for EBPR, *Water Res.*, 42(3) (2008) 557–566.
- [26] H. Monclús, J. Sipma, G. Ferrero, J. Comas, I. Rodriguez-Roda, Optimization of biological nutrient removal in a pilot plant UCT-MBR treating municipal wastewater during start-up, *Desalination*, 250 (2010) 592–597.
- [27] X. Zheng, R. Wu, Y. Chen, Effects of ZnO nanoparticles on wastewater bio-logical nitrogen and phosphorus removal, *Environ. Sci. Technol.*, 45(7) (2011) 2826–2832.